HHS Public Access

Author manuscript

Cell Rep. Author manuscript; available in PMC 2023 December 19.

Published in final edited form as:

Cell Rep. 2023 October 31; 42(10): 113188. doi:10.1016/j.celrep.2023.113188.

Melanocortin-3 receptor expression in AgRP neurons is required for normal activation of the neurons in response to energy deficiency

Yijun Gui[1,2], **Naima S. Dahir**[1,3], **Yanan Wu**[1,2], **Griffin Downing**[1,2], **Patrick Sweeney**[4], **Roger D. Cone**[1,2,3,5,*]

[1]Life Sciences Institute, University of Michigan, Ann Arbor, MI 48109-2216, USA

[2]Department of Molecular, Cellular, and Developmental Biology, University of Michigan, Ann Arbor, MI 48109-2216, USA

[3]Department of Molecular and Integrative Physiology, University of Michigan, Ann Arbor, MI 48109-2216, USA

[4]Department of Molecular and Integrative Physiology, University of Illinois, Urbana-Champaign, IL 61801-3633, USA

[5]Lead contact

SUMMARY

The melanocortin-3 receptor (MC3R) is a negative regulator of the central melanocortin circuitry via presynaptic expression on agouti-related protein (AgRP) nerve terminals, from where it regulates GABA release onto secondary MC4R-expressing neurons. However, MC3R knockout (KO) mice also exhibit defective behavioral and neuroendocrine responses to fasting. Here, we demonstrate that MC3R KO mice exhibit defective activation of AgRP neurons in response to fasting, cold exposure, or ghrelin while exhibiting normal inhibition of AgRP neurons by sensory detection of food in the *ad libitum*-fed state. Using a conditional MC3R KO model, we show that the control of AgRP neuron activation by fasting and ghrelin requires the specific presence of MC3R within AgRP neurons. Thus, MC3R is a crucial player in the responsiveness of the AgRP soma to both hormonal and neuronal signals of energy need.

In brief

*Correspondence: rcone@umich.edu.

AUTHOR CONTRIBUTIONS

Y.G., P.S., and R.D.C. designed the experiments. Y.G., N.S.D., and Y.W. performed experiments, and Y.G. and R.D.C. analyzed the data. G.D. generated MC3R$^{flox/flox}$ mice. Y.G. and R.D.C. wrote the manuscript.

DECLARATION OF INTERESTS

R.D.C., P.S., and the University of Michigan have equity in Courage Therapeutics, and R.D.C. serves on the board of the company. R.D.C. and P.S. have patents filed related to drug development based on the MC3R.

INCLUSION AND DIVERSITY

One or more of the authors of this paper self-identifies as an underrepresented ethnic minority in their field of research or within their geographical location. One or more of the authors of this paper self-identifies as a member of the LGBTQIA+ community.

SUPPLEMENTAL INFORMATION

Supplemental information can be found online at https://doi.org/10.1016/j.celrep.2023.113188.

Gui et al. reveal the role of MC3R in appetite control by regulating the activation of AgRP neurons in response to diverse signals of energy deficiency. Much of this effect involves a direct role of MC3R in the AgRP neuron.

Graphical Abstract

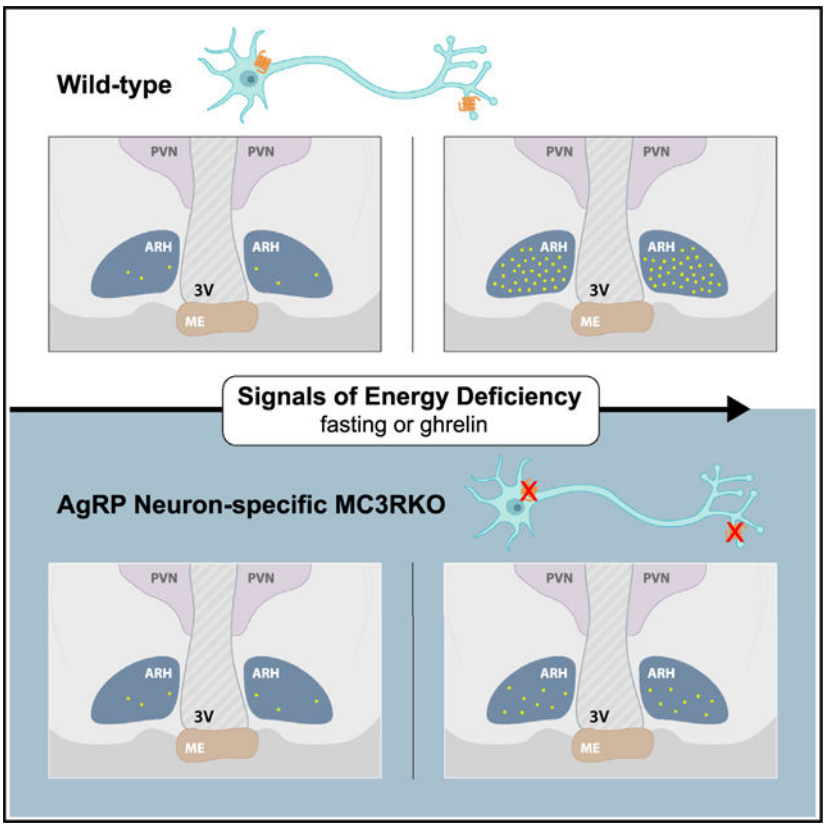

INTRODUCTION

The central melanocortin system, consisting of the primary melanocortinergic AgRP and proopiomelanocortin (POMC) neurons in the arcuate nucleus (ARC) and the downstream target sites expressing the melanocortin-3 or −4 receptors (MC3Rs/MC4Rs), is critical for the maintenance of energy homeostasis.[1] The mechanistic link between MC4R deficiency and obesity is well established,[2–4] with the MC4R being critical for the establishment of adipostasis, in part via its role in communicating the leptin signal to the CNS.[5] In contrast, MC3R deficiency in mouse causes no hyperphagia and mild, late-onset obesity.[6,7] One major mechanism functionally distinguishing MC3R from MC4R lies in their distinct expression patterns in the brain,[8,9] with *MC3R*, but not *MC4R*, exhibiting dense mRNA expression in the AgRP and POMC neurons.[10] The MC3R was demonstrated to act presynaptically on AgRP neurons, where it regulates GABA release from these terminals onto downstream sites expressing MC3Rs and/or MC4Rs.[11] Chemogenetic manipulation of the ARC MC3R neurons or the pharmacological manipulation of the central MC3R circuitry bidirectionally regulates food intake in a manner phenocopying the manipulation of

AgRP neurons.[12] Further, it has been demonstrated experimentally that the MC3R regulates GABA release onto both POMC neurons[13] and paraventricular nucleus of the hypothalamus (PVN)-MC4R neurons.[11] Collectively, these data support the model that the MC3R in AgRP terminals may have a global role providing negative regulatory feedback to the entire melanocortin system. Indeed, MC3R knockout (KO) mice are hypersensitive to both MC4R agonists[11] and anorexigenic behavioral stimuli,[12] yet they also exhibit increased obesity when fed a high-fat diet,[11] and this has led to the concept that the MC3R is required for the regulation of the upper and lower boundaries of energy homeostasis rather than the set point itself. However, the MC3R is also required for normal neuroendocrine and behavioral response to fasting,[14,15] and the mechanism(s) underlying these observations have not been explained. While MC3R KO mice exhibit normal amounts of *ad libitum* feeding, a deficit in fast-induced refeeding is readily visible and persists for many days after a single overnight fast.[11] MC3R KO mice also exhibit a defect in fasting-induced activation of the hypothalamic-pituitary-adrenal axis,[14] fasting-induced suppression of the thyroid axis,[12] and fasting-induced suppression of the hypothalamic-pituitary-gonadal axis.[16] Absence of the MC3R has also been demonstrated to suppress linear growth and pubertal maturation in both mouse and human.[6,7,14,16] Here, we identify cellular and molecular mechanisms for the regulation of the fasting response by the MC3R.

RESULTS

MC3R is required for the activation of AgRP neurons by fasting

Both male and female MC3R KO mice exhibited defective refeeding in response to a 24-h fast compared with their wild-type (WT) littermates (Figures 1A–1D), as shown previously.[11,14] We next examined hypothalamic mRNA expression by qPCR over a 48-h-fasting time course in both sexes. We found that compared with WT controls, both male and female MC3R KO mice demonstrated significantly impaired fasting-induced upregulation of AgRP and neuropeptide Y (NPY) mRNA levels over the entire course of 48-h fasting, while the POMC mRNA levels between the two groups were comparable (Figures 1E–1J). Despite relatively reduced expression, there was still a marked upward trend of AgRP and NPY mRNA levels in MC3R KO mice upon fasting, suggesting that the activation of AgRP neurons in MC3R KO mice was suppressed but not fully abolished.[15]

To further investigate the impaired activation of AgRP neurons in MC3R KO mice, we next performed cFos immunostaining in the arcuate nucleus of NPY-GFP mice, as an indicator of neuronal activation, using NPY-GFP expression as a marker of AgRP neurons. Compared with the WT group, MC3R KO male and female mice exhibited significantly fewer cFos-positive AgRP neurons in response to a 24-h fast but not under *ad libitum* (*ad lib*)-fed conditions (Figures 1K, 1L, S1A, and S1D−S1E). MC3R KO and WT mice had comparable numbers of total AgRP neurons regardless of the feeding state (Figures 1M and S1B). Previous work has shown that both AgRP and non-AgRP GABAergic neurons in the ARC can be activated by fasting.[17] Given the expression of MC3R mRNA detected in non-AgRP cells in the ARC,[12,18] we next examined whether fasting activated MC3R-positive non-AgRP neurons in the ARC. While a significant increase in cFos immunoreactivity

was seen in non-AgRP MC3R-positive ARC cells following fasting, this increase in cFos immunoreactivity was also diminished in the absence of the MC3R (Figure S1C).

Defective AgRP neuron activation in fasted MC3R KO mice is not a result of developmental adaptation or differential reduction in leptin

To explain impaired AgRP neuron activation in fasted MC3R KO mice, one possibility is that such a defect is a result of developmental adaptions to MC3R loss. Although a previous study showed that defective fasting-induced refeeding can be reproduced via knockdown of arcuate *MC3R* expression in adult mice,[11] the activation of AgRP neurons was not examined. To test this, here we performed viral-mediated knockdown of *MC3R* by injecting adeno-associated virus (AAV)-coding short hairpin RNA (shRNA) against *MC3R* or a scrambled control sequence unilaterally in the ARC of adult WT male mice (Figure S2A). Following shRNA expression, we performed cFos immunostaining to compare the number of fasting-activated neurons in the viral injection side versus the control side (Figure S2B). In scramble shRNA-expressing mice, cFos signals were equally expressed in the two sides regardless of fed or fasted state. In *MC3R* shRNA-expressing mice, however, fasting-induced cFos expression was significantly less in the viral injection side compared with in the control side (Figures S2C and S2D). These results suggested that the impaired AgRP neuron activation in MC3R KO mice could be recapitulated by ARC *MC3R* knockdown in adulthood. Therefore, the defective fasting-induced activation of AgRP neurons is not a result of developmental adaptations to MC3R loss. Notably, despite normal body weight compared with scramble shRNA-expressing mice, MC3R shRNA-expressing mice exhibited decreased fat mass percentage and increased lean mass percentage (Figures S2E−S2G), consistent with a role of arcuate MC3R as a negative regulator of the anorexigenic melanocortin circuits.

Another possibility that could explain the defective AgRP neuron activation in the absence of MC3R is that fasted MC3R KO mice have a defect in fat utilization. In response to fasting, adipose tissues undergo lipolysis to provide sources as energy fuel, accompanied by a decrease in plasma leptin levels.[19] Previous work has shown that such a decrement in leptin levels is critical for AgRP neuron activation during fasting.[20] To test for a defective fast-induced mobilization of adipose mass, we measured fasting-induced changes in fat mass and leptin levels in MC3R KO and WT male mice. Despite hyperleptinemia, we found that MC3R KO mice exhibited a comparable decrease in plasma leptin levels in response to a 24-h fast compared with the WT group (Figures S2H, S2I, and S2L). In addition, the linear regression analysis of decreased fat mass and decreased leptin levels during fasting demonstrated comparable results between MC3R KO and WT groups (Figures S2J and S2K), further suggesting that MC3R KO mice have normal fasting-induced fat utilization. In AgRP-specific MC3R KO mice, which will be described further in detail, we also observed equal plasma leptin levels and comparable linear relationships between leptin levels and fat mass compared with the control group (Figures S2M and S2N). Taken together, our data suggested that defective AgRP neuron activation in fasted MC3R KO mice is not a result of differential reduction in leptin.

MC3R is required for the activation of AgRP neurons in response to cold

Cold exposure is another example of energy need that evokes adaptive hyperphagia as a compensation for the increased heat production.[21,22] While much is known regarding the neurocircuitry underlying cold-induced thermogenesis,[23,24] the involvement of AgRP neurons in the regulation of cold-induced hyperphagia had not been discovered until recently.[25,26] Given the role of MC3R in regulating AgRP neuron activation by fasting, we tested if MC3R is also required for the cold-induced activation of AgRP neurons. Similarly, we found that both male and female MC3R KO mice exhibited defective hyperphagia compared with WT mice following 4-h cold exposure (4°C versus 22°C) (Figures 2A and 2D). Cold-induced upregulation of AgRP and NPY mRNA levels was largely blunted in MC3R KO mice in both sexes (Figures 2B and 2E). In WT mice, a significant drop in body temperature was detected in response to cold challenge (Figures 2C and 2F), while MC3R KO males, but not females, showed significantly higher body temperature following cold exposure, indicating increased thermogenesis despite reduced energy intake in the absence of MC3R.

We next performed cFos immunostaining and fiber photometry to directly examine AgRP neuron activity following cold exposure. Compared with WT mice, which demonstrated evident cold-induced cFos expression in AgRP neurons, both MC3R KO male and female mice showed significantly less cFos signal following cold exposure (Figures 2G, 2H, S3A, and S3B). To measure calcium activity in AgRP neurons, AgRP-IRES-Cre mice were crossed to the MC3R KO line and received a unilateral injection of pAAV5-Syn-Flex-GCaMP6s-WPRE-SV40 virus in the ARC, followed by implantation of an optical fiber above the injection site. The accuracy of viral expression was further validated (Figure 2J).

Freely moving male mice were acclimated to a temperature-controlled metal plate before the fiber photometry experiment (Figure 2I). During recording, temperature of the plate was set to decrease from room temperature (room temp) to a cold temperature (12°C), with a 30-s ramp time in transition. In accordance with previous findings,[25,26] we found that AgRP neuron activity in WT animals rapidly increased following the drop in environmental temperature. However, such a cold-induced increase in AgRP neuron activity was greatly blunted in MC3R KO mice (Figures 2K−2M). Consistent with previous data,[25,26] although cold exposure induced an immediate and sharp increase in AgRP neuron activity, we could not observe a sustained neuronal activation throughout the duration of the cold (Figure 2L). Together, these findings suggest that MC3R is required for the activation of AgRP neurons in sensing different forms of energy need, including not only food deprivation but also cold challenge.

MC3R is not required for the inhibition of AgRP neurons by sensory detection of nutrients in the *ad lib*-fed state

Having demonstrated the role of MC3R in regulating AgRP neuron activation by signals of energy need, we next asked if MC3R is also required for the inhibition of AgRP neurons in response to nutrients or food cues, as shown previously.[27–30] We first investigated how MC3R deletion affects inhibition of AgRP neurons in *ad lib*-fed mice in response to delivery of intragastric nutrients. To this end, we performed oral gavage of Ensure and recorded

calcium activity in AgRP neurons by fiber photometry. As previously described for WT mice,[27,30] intragastric nutrient detection rapidly and durably inhibited AgRP neuron activity in a caloric-dependent manner. We found that in response to either 30% or 100% Ensure gavage, MC3R KO mice exhibited a comparable decrease in AgRP neuron activity to WT mice (Figures 3A–3C).

We next examined how MC3R deletion affects inhibition of AgRP neurons in fasted mice in response to either caged or accessible chow. We paired 24-h-fasted WT and MC3R KO mice and performed fiber photometry to record AgRP neuron activity. We found that compared with the WT group, MC3R KO mice fasted for an equal period of time exhibited less decrease in AgRP neuron activity in response to food cues. In WT mice, subsequent presentation of accessible chow further inhibited AgRP neurons, while in MC3R KO mice, there was no difference between the caged- and the accessible-chow-induced inhibitions (Figures 3D–3F).

A caveat to the 24-h-fasting data, however, is that the extent of AgRP neuronal activation differs between WT and MC3RKO mice, as indicated by the mRNA analysis from Figures 1E–1J. Thus, the minor inhibition of AgRP neurons by food detection in MC3R KO mice can be explained by two mechanisms. One possible explanation is that the inhibition of AgRP neurons by external sensory cues is impaired in MC3R KO mice. Alternatively, AgRP neurons in fasted MC3R KO mice are not activated to the same extent as in fasted WT controls, thereby exhibiting less inhibition. To attempt to repeat this experiment under conditions in which AgRP neurons are comparably activated in the two groups, we repeated the analysis comparing 12-h-fasted WT with 36-h-fasted MC3R KO mice, given that they exhibited comparable upregulation of AgRP mRNA levels under these conditions (Figure 1E). We found that in response to “caged” or accessible food pellets, 36-h-fasted MC3R KO mice exhibited equal levels of decrease in AgRP neuron activity compared with the 12-h-fasted WT group (Figures 3G–3I). These results suggested that despite compromised activation of AgRP neurons in the absence of MC3R, MC3R KO mice exhibit intact kinetics of AgRP neuron inhibition by sensory detection of food. Taken together, our data suggested that MC3R may not be required for the inhibition of AgRP neurons by sensory detection of nutrients or food cues.

MC3R deletion in AgRP neurons alone impairs sensing of energy deficiency

Given the expression of *MC3R* transcripts in nearly all AgRP neurons,[12] we next asked if control of AgRP neuron activation requires the specific presence of MC3R within AgRP neurons. To this end, we first attempted to validate MC3R protein existence by examining its expression in AgRP cell bodies and AgRP nerve terminals in the PVN. Since no validated MC3R antibodies are available, we unilaterally injected Cre-dependent virus encoding a FLAG-tagged MC3R protein into the ARC of AgRP Cre mice. Immunohistochemical detection of FLAG expression colocalized with AgRP cell bodies in the ARC and with AgRP nerve terminals in the PVN by immunostaining (Figures 4A and 4B).

Next, we sought to specifically delete MC3R in AgRP neurons by crossing AgRP-Cre with MC3R-flox mouse lines to generate a tissue-specific MC3R KO model. Using RNAScope *in situ* hybridization, we validated KO efficiency by showing *MC3R* deletion in ~70%

of AgRP neurons (Figures 4C and 4D). We then interrogated whether the mild obesity and the defective fasting responses in global MC3R KO mice could be recapitulated by AgRP-specific deletion of MC3R. We found that AgRP-specific MC3R KO male mice exhibited increased body weight and decreased lean mass percentage compared with the AgRP-Cre control group (Figures 4E–4G), which phenocopied the global MC3R KO model.[6,7] In AgRP-specific MC3R KO females, however, there was no difference in their body composition compared with the control group (Figures S4A−S4C). In response to fasting, we found that both male and female AgRP-specific MC3R KO mice showed defective cFos expression in the ARC, while only males, but not females, demonstrated blunted refeeding behavior compared with the control group (Figures 4H–4J and S4D-S4F). Similarly, in response to cold exposure, although we observed a trend toward reduced cFos expression in the ARC in both male and female AgRP-specific MC3R KO mice, only males, but not females, demonstrated defective cold-induced hyperphagia compared with controls (Figures 4K−4M, and S4G−S4I).

Upon fasting, significant changes occur in adrenal, gonadal, and thyroidal axes.[31] Previous work has shown that in response to a 36-h fast, the suppression of thyroid hormone (total T4) levels is greatly impaired in MC3R global KO mice compared with in the WT group.[11] Here, we also measured serum levels of total T4 in AgRP-specific MC3R KO male mice and their controls in response to fasting. We found that fasting induced a significant decrease in total T4 levels in both groups, and total T4 was not significantly different in AgRP-specific MC3R KO and AgRP-Cre mice in basal fed or fasted states (Figures S5A and S5B). Thus, our data suggest that despite the recapitulation of defective AgRP neuron activation and hyperphagia, AgRP-specific MC3R KO mice still exhibit normal fasting suppression of the thyroid axis.

MC3R regulates downstream MC4R-mediated anorexigenic activity thorough its action in AgRP neurons

Previous electrophysiological data supported that MC3R is required for GABA release from AgRP neuron terminals onto downstream PVN-MC4R neurons,[11] implying the role of MC3R as a negative regulator of the MC4R circuitry. In line with this, global MC3R KO mice exhibited hypersensitivity to MC4R agonists.[11] We then sought to examine the effect of AgRP-specific MC3R deletion on MC4R-mediated anorexigenic responses. To this end, we chose setmelanotide, an FDA-approved MC4R agonist drug for treatment of POMC and leptin receptor deficiency,[32] and tested its anorexigenic action over a 24-h time course following injection. Compared with the control group, the administration of setmelanotide (2 mg/kg, intraperitoneally [i.p.]) in AgRP-specific MC3R KO male mice generated more robust and longer-lasting effects in food intake suppression at all time points measured after 1 h (Figure 5A). Consistently, setmelanotide induced more profound weight loss in AgRP-specific MC3R KO males compared with the control group (Figure 5B). In females, however, we found that there was no significant difference of food intake or body weight between AgRP-specific MC3R KO mice and the control group in response to setmelanotide administration (Figures 5C and 5D). Together, our findings confirmed the hypersensitivity of downstream anorexigenic MC4R neurons in the absence of MC3R in AgRP neurons in male mice.

MC3R is required for the orexigenic action of ghrelin on AgRP neurons

We next investigated the mechanisms underlying defective AgRP neuron activation in the absence of MC3R. Ghrelin is an important hormonal signal of energy state that regulates AgRP neuron activity.[33] Inadequate sensing of ghrelin could be one of the mechanisms underlying defective AgRP neuron activation due to MC3R deletion. Previous work has shown that compared with WT mice, global MC3R KO mice exhibit normal serum ghrelin levels but eat significantly less in response to ghrelin injection.[34] Here, we first sought to confirm the requirement of AgRP-specific MC3R expression for such ghrelin-induced hyperphagia. To this end, we examined food intake following peripheral ghrelin administration in the presence and absence of MC3R in AgRP neurons in both sexes. In male mice, the acute hyperphagia induced by ghrelin injection (1.6 mg/kg, i.p.) was greatly diminished in AgRP-specific MC3R KO mice compared with the control group (Figure 6A), confirming that MC3R is required for the orexigenic effect of ghrelin through its specific presence in AgRP neurons. In female mice, however, the food intake was not significantly different in the conditional MC3R KO group and controls (Figure S6A). We next examined the activation of AgRP neurons by ghrelin in the presence and absence of MC3R. We performed cFos immunostaining and found that ghrelin-induced cFos expression in the ARC was significantly suppressed in AgRP-specific MC3R KO male mice, but not in females, compared with the control group (Figures 6B, 6C, S6B, and S6C).

We then performed fiber photometry to record calcium signals in AgRP neurons in response to ghrelin (Figure 6D). In WT mice, as previously described, ghrelin administration (1.6 mg/kg, i.p.) induced a rapid and robust increase in AgRP neuron activity, which was greatly suppressed by subsequent sensory detection of a chow pellet (Figures 6E–6H).[28] In MC3R KO mice, however, we found a significant impairment in ghrelin-induced increase in AgRP neuron activity (Figures 6E–6G) and, accordingly, less inhibition by subsequent food presence (Figures 6E and 6H).

We next investigated the effect of MC3R deletion on ghrelin receptor expression under *ad lib*-fed and fasted states. We first performed qPCR analysis of *Ghsr* mRNA levels and found that compared with the WT group, MC3R KO mice exhibited significantly less upregulation of *Ghsr* expression in the hypothalamus upon fasting (Figure 6I). We also performed RNAScope *in situ* hybridization to examine the levels of *Ghsr* mRNA in AgRP neurons in AgRP-specific MC3R KO versus AgRP-Cre control mice (Figures 6J−6L). In the control group, fasting significantly increased the number of *Ghsr* transcripts in AgRP neurons and the percentage of AgRP neurons expressing *Ghsr* (Figures 6K and 6L). In the AgRP-specific MC3R KO group, however, there was an evident defect in fasting-induced *Ghsr* upregulation in AgRP neurons (Figures 6K and 6L). Together, these findings suggested that MC3R deletion from AgRP neurons leads to impaired responses to ghrelin, concomitant with a defect in fasting-induced upregulation of *Ghsr* mRNA levels in AgRP neurons.

MC3R is required for excitatory synapse-associated gene expression in AgRP neurons

Upon food deprivation, excitatory synaptic plasticity occurs in AgRP neurons.[35,36] Previous RNA sequencing analysis also revealed significant changes in expression of genes associated with glutamate signaling and synaptic plasticity in AgRP neurons during fasting.[37]

For example, α-amino-3-hydroxy-5-methyl-4-isoxazolepropionic acid (AMPA) glutamate ionotropic receptors mediate excitatory synaptic transmission, and *Gria3* encoding AMPA receptor subunit 3 (GluA3) was found significantly upregulated in AgRP neurons upon fasting.[37] Proline-rich tyrosine kinase 2 (Pyk2) plays an important role in spine morphology and excitatory synaptic plasticity,[38,39] and its gene *Ptk2b* was also found to be greatly upregulated in AgRP neurons during fasting.[37] Here, we sought to examine fasting-induced expression of these two excitatory synapse-associated genes, *Gria3* and *Ptk2b*, in AgRP neurons in the presence and absence of MC3R.

We performed RNAScope *in situ* hybridization and found that in the control group, fasting significantly increased the number of *Gria3* and *Ptk2b* transcripts in AgRP neurons, as well as the percentage of AgRP neurons expressing them (Figures 7A–7E). In the AgRP-specific MC3R KO group, however, the upregulation of *Gria3* and *Ptk2b* transcript numbers by fasting was greatly reduced in AgRP neurons (Figures 7A, 7B, 7D, and 7E). Although the percentage of AgRP neurons expressing *Gria3* was comparable in AgRP-specific MC3R KO mice compared with controls, there was a significant suppression in the percentage of *Ptk2b*-positive AgRP cells in conditional KO versus control groups upon fasting (Figures 7C and 7F). Taken together, our data suggested that MC3R deletion in AgRP neurons impairs the upregulation of excitatory synapse-associated genes upon fasting, which can be one mechanism underlying failed AgRP neuron activation in the absence of MC3R.

DISCUSSION

In this study, we demonstrate a role for MC3R in regulating AgRP neuron activation in male and female mice in response to two different paradigms of energy demand: food deprivation and cold exposure. The data here show a clear requirement of MC3R expression within AgRP neurons for the normal activation of these cells in response to nutritional deficit in both male and female mice. The successful recapitulation of defective fasting responses in AgRP-specific MC3R KO mice demonstrates the dominant effect of MC3R in AgRP neurons across the entire melanocortin circuitry regulating feeding behavior. These findings are consistent with recent data showing the dominance of the orexigenic activity of AgRP neurons over anorexigenic POMC neurons.[40] This finding, in turn, helps explain the multiple observations of defective fast-induced behavioral and neuroendocrine responses to fasting reported in the MC3R KO mouse.[11,14–16] We found that despite the requirement of MC3R for AgRP neuron activation, MC3R is dispensable for the inhibition of AgRP neurons by nutritional gavage in the *ad lib*-fed state, likely understood in terms of the different mechanism(s) by which AgRP neurons are activated versus deactivated.[27]

Male and female mice lacking MC3R specifically in AgRP neurons exhibited comparable decreases in AgRP activation when fasted, as indicated by reduced cFos positivity in AgRP neurons. Males lacking MC3R specifically in AgRP neurons exhibited defective hyperphagia when exposed to cold and a non-significant trend toward decreased activation of AgRP neurons, while females exhibited a small and non-significant trend in AgRP neuron activation and no hyperphagic response. Since global MC3R deletion blunted cold-induced hyperphagia and AgRP neuron activation in males and females, these data suggest that non-AGRP MC3R neurons may also play a role in cold-induced feeding responses.

Other phenotypes observed in males lacking MC3R in AgRP neurons were not observed in females, including increased adipose mass and reduced lean mass, reduced fast-induced refeeding, and reduced ghrelin sensitivity. It is possible that these phenotypes may become observable if the female animals are comparably staged in the reproductive cycle. However, despite comparably dense expression of MC3R transcripts in AgRP neurons in both males and females, MC3R exhibits significant sexually dimorphic expression in multiple other hypothalamic nuclei that are downstream of AgRP and POMC innervation.[18] For example, the number of MC3R neurons is significantly higher in the anteroventral periventricular nucleus hypothalamus (AVPV), the principal nucleus of the bed nucleus of the stria terminalis (BSTPr) and ventral premammillary nucleus (PMv). Therefore, it is possible that the phenotypes we observed in global, but not AgRP-specific, MC3R KO female mice largely result from MC3R loss in the nuclei mentioned above, while the phenotypes in MC3R KO male mice result from MC3R loss in mainly AgRP neurons. Such a sexually dimorphic pattern of MC3R expression can potentially account for the discrepancy we observed between defective AgRP neuron activation by fasting yet normal fast-induced refeeding behavior in AgRP-specific MC3R KO females. Thus, it is fascinating to speculate that female mice have compensatory MC3R circuits that can respond to reduced AgRP activity in ways not available to male mice.

While the cellular basis for the effects of MC3R on the fasting response is described here, involving MC3R expression within AgRP neurons, the molecular basis of MC3R action on the AgRP soma remains unknown and could involve either presynaptic and/or postsynaptic mechanisms of MC3R action. The presynaptic actions of the MC3R have been demonstrated with slice electrophysiological studies, showing a role for the MC3R in stimulating GABA release from AgRP terminals onto both downstream melanocortin receptor-expressing cell types tested, the MC3R-expressing POMC neurons[13] and the PVN-MC4R neurons.[11] The data presented here show that AgRP neurons are still partially activated by fasting in the absence of MC3R function but that they exhibit greatly reduced sensitivity to signals of nutritional deficit, known to be mediated through both hormonal (e.g., leptin and ghrelin) and neuronal inputs. Leptin levels are sensed not only by AgRP neurons but also a through a network of LepRb-expressing GABAergic neurons[41] such as the GABAergic dorsomedial hypothalamic LepRb neurons known to densely innervate AgRP neurons.[42] The results shown here are consistent, for example, with increased GABAergic tone on the AgRP neurons, which could result if there are reciprocal connections between AgRP neurons, and other LepRb-expressing GABAergic neurons, with reduced GABAergic drive from MC3R-deficient AgRP terminals. Of note, previous work has also demonstrated the potentiation of excitatory $PVN^{TRH} \rightarrow$ AgRP synapses upon caloric deficit, which promotes the activation of AgRP neurons and drives feeding behavior.[43,44] Here, our data suggest that MC3R is required for the upregulation of excitatory synapse-associated genes upon fasting, which can provide yet another molecular mechanism for reduced AgRP neuron activation in the absence of MC3R.

While we show here that a tagged MC3R is expressed in AgRP soma, there are few other data to support a postsynaptic role for the MC3R on AgRP soma. Innervation of AgRP cell bodies by POMC or AgRP fibers has not been reported, and no responses were observed in AgRP cell bodies following optogenetic stimulation of POMC or AgRP neurons.[45] Further,

direct application of a broad melanocortin agonist, MTII, to AgRP cells was not seen to alter the activity of these neurons,[46] although the endogenous antagonist of the MC3R and MC4R, AgRP, was not tested, nor was a neuromodulatory role for MC3R in response of the cells to fast neurotransmitters. Thus, additional work is required to determine if endogenous MC3R is actually expressed on AgRP soma, what the source of the ligand is, and how this may impact neuronal activation.

Remarkably, the deletion of a number of different receptors and receptor accessory proteins from AgRP neurons, including the NMDA receptor,[35] the growth hormone receptor,[47] and the G protein-coupled receptor (GPCR) accessory protein MRAP2[48] all blunt the responsiveness of AgRP neurons to fasting-induced activation. The observation that deletion of any one of several different receptors or receptor accessory proteins from AgRP neurons (MC3R, GHR, MRAP2, NMDAR) each can blunt fasting-induced activation may suggest that these molecules are part of a complex signaling system. However, given the specificity of expression of the MC3R within the central melanocortin system, the results shown here make the MC3R a potential drug target for blocking weight regain, since MC3R-specific antagonists could be expected to blunt the behavioral and neuroendocrine responses to weight loss, regardless of whether such loss results from pharmacotherapy, or diet and exercise.

Limitations of the study

In this study, we have used global and tissue-specific deletion of the MC3R to characterize functions of this receptor, and thus it is possible that some phenotypes result from developmental activities of the receptor. However, we control for this by showing that knockdown of the ARC MC3R in adult mice also blunts fasting-induced activation of cFos in the ARC (Figure S1). We showed sexual dimorphism between male and female AgRP-specific MC3R KO mice, while *Mc3r* deletion efficiency was only examined in male conditional KO mice. It is possible that insufficient deletion of *Mc3r* or developmental adaptations may result in the failed recapitulation of phenotypes in female mice. While expression of MC3R protein in MC3R soma in the ARC can be shown by viral overexpression, this does not prove that the endogenous MC3R is functionally expressed on AgRP soma. Ultimately, slice electrophysiology of AgRP neurons will be needed to determine if endogenous MC3R is functionally expressed on MC3R soma and to potentially determine the identity of the endogenous ligand and signaling mechanisms.

STAR★METHODS

RESOURCE AVAILABILITY

Lead contact—Further information and requests for resources and regents should be directed to and will be fulfilled by the Lead Contact, Dr. Roger D. Cone (rcone@umich.edu).

Materials availability—This study did not generate reagents. Commercially available reagents are indicated in the Key resources table. This study generated one animal strain, the MC3R flox/flox mouse, which may be requested from the lead contact.

Data and code availability

- This study did not generate standardized data types. Data will be made available by the lead contact upon request.
- This paper does not report original code.
- Any additional information required to reanalyze the data reported in this paper is available from the lead contact upon request.

EXPERIMENTAL MODEL AND STUDY PARTICIPANT DETAILS

Animals—Experiments were performed on adult (12–16 weeks old) male and female mice. In this study, mouse strains including C57/BL6J (Jax: 000664), AgRP-IRES-Cre (Jax: 012899), NPY-hrGFP (Jax: 006417), Ai14 (Jax: 007914) and EGFP-L10a (Jax: 024750) were obtained from Jackson Laboratories. age. MC3R KO mice were generated and maintained in a C57BL/6 background as previously described.[7]

The creation of MC3R flox/flox (MC3R fl/fl) mice is reported here. Briefly, MC3R fl/fl mice were made by inserting *loxP* sites to flank the single exon using a guide RNA (gRNA) to the Mc3R gene, with the donor vector containing the *loxP* sites (Cyagen, Inc). The 5′ *loxP* site is inserted into 5′ UTR and the 3′ *loxP* site sits after the 3′ UTR. The gRNA (target sequence: AAGAGTTCATGGTTAACAGCAGG) was co-injected with Cas9 to generate conditional knockout offspring. Founder animals were then bred to wild type to test for germline transmission. F1 heterozygous mutants were identified by additional PCR screening using two sets of primers: 5′arm forward primer (F2): 5′-GTTCATCTGTCTAGCAGCTTCATT-3′ 3′*loxP* reverse primer (R2): 5′-GTGGATTCGGACCAGTCTGA-3, and 5′*loxP* forward primer (F1): 5′-ACGTAAACGGCCACAAGTTC-3′ 3′arm reverse primer (R1): 5′-TTATCCACCACACCTTGCTTTCTC-3’. For sequencing confirmation, additional PCR was conducted using 2 sets of primers: Sequencing Primer for PCR product 1: 5′Sequence primer (R4): 5′-GATAAACTGGTCCTCCAAGGTCAG-3′ Sequencing Primer for PCR product 2: 3′Sequence primer (R3): 5′-GGTA GAATCTCCTTGTGTGTGTTT-3’. MC3R $^{fl/fl}$ mice were bred to AgRP-Cre to produce AgRP-specific MC3R KO mice (AgRP Cre $^{+/-}$, MC3R $^{fl/fl}$). All experiments were previously approved by the University of Michigan Institutional animal care and use office (IACUC).

METHOD DETAILS

Food intake studies—For all feeding and behavioral assays mice were matched for gender, age, and body weight. Gender differences in behavioral assays are depicted in either the main text or the supplementary figures. Mice were provided with *ad libitum* access to food and water in temperature-controlled (22°C) rooms on a 12 h light-dark cycle with daily health status checks. For feeding assays mice were single housed for at least two weeks before starting feeding measurements. Food pellets were provided in a wire feeder, and intake was measured manually including all crumbs or measured by the FED3 device.

Fast-refeeding assays—12 to 16-week-old WT and MC3R KO male and female mice were fasting for 24 h. Right before the dark cycle, a weighed amount of food was provided,

and the food was weighed again 2hr, 4hr, 8hr and 24hr after refeeding. Food intake was calculated as the difference in food weight over the 24hr refeeding time course, and was compared to the *ad lib* fed food intake in the same time period.

Cold exposure feeding assays—Single-cage housed WT and MC3R KO mice were habituated to the temperature-controlled chamber at room temperature (22°C) for 3 days prior to the test. For the cold-induced feeding experiment, mice were maintained in the chamber at 4 or 22°C with free access to food and water for 4hr in the light cycle. The food was weighted right before and after the cold exposure.

Real-time PCR analyses—To measure the gene expression of AgRP, NPY, POMC and GHSR, WT or MC3R KO mice were *ad lib* fed or fasted for 12, 24, 36 and 48 h from the beginning of the dark cycle. To measure the gene expression in response to cold exposure, acclimated mice were maintained in the chamber at 4 or 22°C with free access to water but food deprived for 4hr in the light cycle. Following fasting or cold exposure, mice were killed and hypothalamic tissue were collected and frozen immediately on dry ice and stored at −80°C. RNA was extracted using TRIzol reagent (Invitrogen), followed by cDNA synthesis using the cDNA reverse transcription kit (Applied Biosystems) according to the manufacturer's instructions. SYBR Green assay was used to examine the gene-expression levels of AgRP, NPY and POMC. Gene expression for each target was normalized to TATA box binding (TBP) gene.

Immunofluorescence and imaging—To measure changes in AgRP neuronal activity in response to fasting or cold exposure, we performed florescent immunohistochemistry to detect cFos and GFP. Mice were euthanized either 24hr after fasting or 2hr after cold treatment and were perfused with 10% formalin. Following perfusion, brains were fixed for an additional 24 h in 10% formalin. Brains were then switched to a 30% sucrose solution (in 1X PBS) until the brains sank in the solution (1–3 days) and at which point 35um thick hypothalamic sections were obtained using a cryostat (Leica). Sections were first incubated for 1 h in blocking buffer (1X PBS with 2% BSA and 0.1% tween 20). Primary antibodies (rabbit anti-cFos, Cell Signaling Technology, 1:500; chicken anti-GFP, Aves Labs, 1:1500) diluted in blocking buffer were added to sections overnight at room temp. After three washes in 1X PBS, secondary antibodies (goat anti-chicken Alexa 488, anti-rabbit Alexa 555, 1:500) diluted in blocking buffer at 1:500 were added to sections for 2 h at room. After three additional wash steps, sections were mounted on slides and imaged on a confocal microscope (Leica SP8). Total number of cFos+ cells, GFP+ cells, cFos+/ GFP+ dual positive cells in the ARC were counted. The percentage of cFos-positive AgRP neurons and GFP-positive cFos cells were calculated accordingly.

For MC3R expression validation experiment, FLAG and AgRP primary antibodies were used and diluted in blocking buffer at 1:200 (mouse anti-FLAG, Sigma) and 1:1000 (rabbit anti-AgRP, Phoenix Pharmaceuticals), respectively. Secondary antibodies (goat anti-mouse Alex 555, anti-rabbit Alexa 647) were diluted in blocking buffer at 1:500 accordingly.

Rectal thermometry—A small-diameter temperature probe was inserted through the anus in WT and MC3R KO mice, with an insertion depth of >2 cm to yield colonic temperatures right before and after cold exposure.

Viral vectors—The adeno associated viral vector pAAV5-Syn-Flex-GCaMP6s-WPRE-SV40 used in this study was purchased from Addgene. The AAV9-CMV-DIO-FLAG-MC3R, AAV2-CMV-MC3R shRNA and AAV2-CMV-scramble shRNA were designed by the University of Michigan Vector Core. The generation and the sequences of the MC3R and scramble shRNAs have been described previously.[10]

Stereotaxic viral injections and fiber placement surgeries—For stereotaxic surgical procedures, 8 to 12-week-old mice were anesthetized with isoflurane and placed in a stereotaxic frame (Kopf). A micro-precision drill was used to drill a small burr-hole directly above the viral injection point and dura was removed. AAV viral vectors of 500nL were injected into the arcuate nucleus using a micromanipulator (Narishige) attached to a pulled glass pipette. Viral injection coordinates for the arcuate nucleus were as follows: A/P: −1.4mm (from bregma), M/L: 0.25mm, D/V: 5.95mm (from surface of the skull). Virus was injected at a rate of 50 nl/min. Following viral injection, the glass pipette was left in place for an additional 10 min to prevent leaking of virus outside the targeted brain region. For fiber implant surgery, after viral injections a fiber-optic ferrule was implanted using the coordinates: A/P: −1.4mm (from bregma), M/L: 0.25mm, D/V: 5.85mm (from surface of the skull). Fibers were attached to the skull using Metabond. Three weeks was allotted post-surgery to allow for viral expression and the mice to recover from surgical procedures. Viral expression and fiber placement were verified post hoc in all animals, and any data from animals in which the transgene expression and/or fiber was located outside the targeted area were excluded from analysis.

Fiber photometry—Mice expressing GCaMP6s in AgRP neurons were connected to a fiber-photometry system to enable fluorometric analysis of realtime neuronal activity. Data were recorded using a Neurophotometrics FP3001 system (Neurophotometrics, San Diego, CA). Briefly, 470 and 415 nm LED light was bandpass filtered, reflected by a dichroic mirror, and focused onto a multi-branch patch cord (Doric, Quebec City, Quebec) by a 20x objective lens. Alternating pulses of 470 and 415 nm light (~50 μW) were delivered at 40 Hz, and photometry signals were analyzed using custom MATLAB scripts. For all recordings, the isosbestic 415 nm excitation control signal was subtracted from the 470 nm excitation signal to remove movement artifacts from intracellular calcium-dependent GCaMP6s fluorescence. Baseline drift was evident in the signal due to slow photobleaching artifacts, particularly during the first several minutes of each recording session. A double exponential curve was fit to the raw trace of temperature-ramping experiments while a linear fit was applied to the raw trace of food presentation experiments and subtracted to correct for baseline drift. After baseline correction, dF/F0 (%) was calculated as individual fluorescence intensity measurements relative to mean fluorescence of the beginning control session for 470 nm channel. In cold exposure experiments, the beginning control session was the −2 to 0 min baseline recording at room temperature. IITC's Incremental Hot/Cold Plate (IITC Life Science) was used to set cold temperature, which requires a 30s ramp time in

transition to drop from room temp to the cold (22°C–12°C). In sensory cue detection and ghrelin response experiments, the beginning control session was the −5 to 0 min baseline recording before any stimulations were presented.

RNAscope fluorescent *in situ* hybridization—To determine the percentage of AgRP neurons that contain Mc3r, Ghsr, Gria3 or Ptk2b and to quantify their mRNA abundance in individual AgRP neurons in the ARC, a RNAscope fluorescent multiplex assay (Advanced Cell Diagnostics) was used. Fresh brain samples were collected, embedded in OCT and frozen immediately on dry ice and stored at −80°C. 18um-thick frozen sections containing the ARC were collected using a sliding microtome and mounted onto Super Frost Plus slides (Fisher Scientific), and *in situ* hybridization was performed according to the RNAscope fluorescent multiplex kit user manual for fresh frozen tissue (Advanced Cell Diagnostics), using RNAscope Probes Mm-Mc3r-C1, Mm-Gria3-C1, Mm-Agrp-C2, Mm-Ghsr-C3 and Mm-Ptk2b-C3. Images of the ARC of each animal were obtained using a laser scanning confocal microscope (Leica SP8). Confocal image stacks were collected through the z axis. Total number of cells (boundary defined by DAPI signals) that co-express AgRP and Mc3r/Ghsr/Gria3/Ptk2b, and the number of each transcript in each AgRP-positive cell were counted manually aided by ImageJ software. Only cells with three times as many fluorescent spots as were measured in background regions, were considered positively labeled for each mRNA transcript.

Body composition—Whole-animal body composition analysis was performed using the Minispec Model mq7.5 (7.5 mHz; Bruker Instruments), which is a benchtop-pulsed 7-T NMR system. The instrument gave lean mass, fat mass, and fluid mass values of the mice, of which the body weight was measured at the same time. The percent of lean or fat mass relative to the whole-body weight was calculated.

Plasma leptin measurements—Plasma leptin levels were measured in 24h-fasted and fed male mice with enzyme-linked immunosorbent assay (Mouse Leptin ELISA Kit, Crystal Chem). Four to five drops of blood were collected in heparinized capillary blood collection tubes (Thermo Fisher Scientific) by tail vein puncture. Blood cells were removed by centrifugation (2000g for 30 min at 4°C), and plasma was flash-frozen for further analysis according to the manufacturer's recommendations.

Total serums T4 measurements—Total serum T4 was measured in 48hr-fasted and fed male mice with enzyme-linked immunosorbent assay (T4 ELISA Kit, Diagnostic Automation). Four to five drops of blood were collected by tail vein puncture and allowed to clot in microfuge tubes for 30 min at room temperature. Then clot was removed by centrifugation (2000g for 10 min at 4°C), and serum was flash-frozen for further analysis according to the manufacturer's recommendations.

Setmelanotide injection—Mice of each genotype (AgRP-speific MC3R KO or AgRP Cre) were weighed and divided into two subgroups, and each subgroup was given either vehicle (200 μL of saline) or setmelanotide (2 mg/kg) in 200 μL of saline by i.p. injection half an hour before the beginning of the dark phase. A weighed amount of food was

provided, and the food was weighed again 2hr, 4hr, 12hr and 24hr after the injection. Mice were weighed again 24hr after injection to calculate the percent change in body weight.

Ghrelin injection—Mice of each genotype (AgRP-speific MC3R KO or AgRP Cre) were weighed and divided into two subgroups, and each subgroup was given either vehicle (200 μL of saline) or ghrelin (1.6 mg/kg) in 200 μL of saline by i.p. injection at 11a.m. during the light phase (7a.m. to 7p.m.). A weighed amount of food was provided, and the food was weighed again 1hr after the injection.

To test ghrelin-induced cFos expression, ghrelin was given by i.p. injection to *ad lib* fed mice at 11a.m. during the light phase (7a.m. to 7p.m.). The food was removed after ghrelin injection while mice had normal access to the water. Two hours following the injection, mice were euthanized and perfused with 1X PBS followed by 10% formalin for further cFos immunostaining experiment as described in the “Immunofluorescence and imaging“ section.

QUANTIFICATION AND STATISTICAL ANALYSIS

Statistical analyses were performed using GraphPad Prism 9.0 software. No statistical method was used to predetermine sample size. For behavioral experiments, n values represent the final number of validated mice. Randomization and blinding methods were not used. Single comparisons between two groups were made by two-tailed unpaired Student’s t-test. Ordinary two-way ANOVA followed by Sidak’s or Tukey’s multiple comparisons test (as recommended) was applied to determine the statistical differences among groups across different time points. All data presented met the assumptions of the statistical test employed. For all statistical tests, $p < 0.05$ was considered significant. Calculated values are presented as mean ± s.e.m. (standard error of the mean), unless indicated otherwise. Statistical significance is represented by * $p < 0.05$, ** $p < 0.01$, *** $p < 0.001$, **** $p < 0.0001$. Statistical tests and parameters are reported in figure legends.

Supplementary Material

Refer to Web version on PubMed Central for supplementary material.

ACKNOWLEDGMENTS

We would like to thank Savannah Y. Williams and Monica Blazevic for their outstanding technical assistance. This work was funded by NIH DK126715 (R.D.C.) and NIH T32 DK101357 (N.S.D.).

REFERENCES

1. Cone RD (2005). Anatomy and regulation of the central melanocortin system. Nat. Neurosci 8, 571–578. [PubMed: 15856065]
2. Huszar D, Lynch CA, Fairchild-Huntress V, Dunmore JH, Fang Q, Berkemeier LR, Gu W, Kesterson RA, Boston BA, Cone RD, et al. (1997). Targeted disruption of the melanocortin-4 receptor results in obesity in mice. Cell 88, 131–141. [PubMed: 9019399]
3. Yeo GS, Farooqi IS, Aminian S, Halsall DJ, Stanhope RG, and O’Rahilly S. (1998). A frameshift mutation in MC4R associated with dominantly inherited human obesity. Nat. Genet 20, 111–112. [PubMed: 9771698]
4. Vaisse C, Clement K, Guy-Grand B, and Froguel P. (1998). A frameshift mutation in human MC4R is associated with a dominant form of obesity. Nat. Genet 20, 113–114. [PubMed: 9771699]

5. Tallam LS, da Silva AA, and Hall JE (2006). Melanocortin-4 receptor mediates chronic cardiovascular and metabolic actions of leptin. Hypertension 48, 58–64. [PubMed: 16754792]
6. Butler AA, Kesterson RA, Khong K, Cullen MJ, Pelleymounter MA, Dekoning J, Baetscher M, and Cone RD (2000). A unique metabolic syndrome causes obesity in the melanocortin-3 receptor-deficient mouse. Endocrinology 141, 3518–3521. [PubMed: 10965927]
7. Chen AS, Marsh DJ, Trumbauer ME, Frazier EG, Guan XM, Yu H, Rosenblum CI, Vongs A, Feng Y, Cao L, et al. (2000). Inactivation of the mouse melanocortin-3 receptor results in increased fat mass and reduced lean body mass. Nat. Genet 26, 97–102. [PubMed: 10973258]
8. Mountjoy KG, Mortrud MT, Low MJ, Simerly RB, and Cone RD (1994). Localization of the melanocortin-4 receptor (MC4-R) in neuroendocrine and autonomic control circuits in the brain. Mol. Endo 8, 1298–1308.
9. Roselli-Rehfuss L, Mountjoy KG, Robbins LS, Mortrud MT, Low MJ, Tatro JB, Entwistle ML, Simerly RB, and Cone RD (1993). Identification of a receptor for gamma melanotropin and other proopiomelanocortin peptides in the hypothalamus and limbic system. Proc. Natl. Acad. Sci. USA 90, 8856–8860. [PubMed: 8415620]
10. Bagnol D, Lu XY, Kaelin CB, Day HE, Ollmann M, Gantz I, Akil H, Barsh GS, and Watson SJ (1999). The anatomy of an endogenous antagonist: relationship between agouti-related protein and proopiomelanocortin in brain. J. Neurosci 19, RC26. [PubMed: 10479719]
11. Ghamari-Langroudi M, Cakir I, Lippert RN, Sweeney P, Litt MJ, Ellacott KLJ, and Cone RD (2018). Regulation of energy rheostasis by the melanocortin-3 receptor. Sci. Adv 4, eaat0866.
12. Sweeney P, Bedenbaugh MN, Maldonado J, Pan P, Fowler K, Williams SY, Gimenez LE, Ghamari-Langroudi M, Downing G, Gui Y, et al. (2021). The melanocortin-3 receptor is a pharmacological target for the regulation of anorexia. Sci. Transl. Med 13, eabd6434.
13. Cowley MA, Smart JL, Rubinstein M, Cerdá n MG, Diano S, Horvath TL, Cone RD, and Low MJ (2001). Leptin activates anorexigenic POMC neurons through a neural network in the arcuate nucleus. Nature 411, 480–484. [PubMed: 11373681]
14. Renquist BJ, Murphy JG, Larson EA, Olsen D, Klein RF, Ellacott KLJ, and Cone RD (2012). Melanocortin-3 receptor regulates the normal fasting response. Proc. Natl. Acad. Sci. USA 109, E1489–E1498. [PubMed: 22573815]
15. Girardet C, Mavrikaki MM, Stevens JR, Miller CA, Marks DL, and Butler AA (2017). Melanocortin-3 receptors expressed in Nkx2.1(+ve) neurons are sufficient for controlling appetitive responses to hypocaloric conditioning. Sci. Rep 7, 44444. [PubMed: 28294152]
16. Lam BYH, Williamson A, Finer S, Day FR, Tadross JA, Gonçalves Soares A, Wade K, Sweeney P, Bedenbaugh MN, Porter DT, et al. (2021). MC3R links nutritional state to childhood growth and the timing of puberty. Nature 599, 436–441. [PubMed: 34732894]
17. Zhu C, Jiang Z, Xu Y, Cai ZL, Jiang Q, Xu Y, Xue M, Arenkiel BR, Wu Q, Shu G, and Tong Q. (2020). Profound and redundant functions of arcuate neurons in obesity development. Nat. Metab 2, 763–774. [PubMed: 32719538]
18. Bedenbaugh MN, Brener SC, Maldonado J, Lippert RN, Sweeney P, Cone RD, and Simerly RB (2022). Organization of neural systems expressing melanocortin-3 receptors in the mouse brain: Evidence for sexual dimorphism. J. Comp. Neurol 530, 2835–2851. [PubMed: 35770983]
19. Caron A, Lee S, Elmquist JK, and Gautron L. (2018). Leptin and brain-adipose crosstalks. Nat. Rev. Neurosci 19, 153–165. [PubMed: 29449715]
20. Takahashi KA, and Cone RD (2005). Fasting induces a large, leptin-dependent increase in the intrinsic action potential frequency of orexigenic arcuate nucleus neuropeptide Y/Agouti-related protein neurons. Endocrinology 146, 1043–1047. [PubMed: 15591135]
21. Andersson B, and Larsson B. (1961). Influence of local temperature changes in the preoptic area and rostral hypothalamus on the regulation of food and water intake. Acta Physiol. Scand 52, 75–89. [PubMed: 13683301]
22. Hamilton CL, and Brobeck JR (1964). Food Intake and Temperature Regulation in Rats with Rostral Hypothalamic Lesions. Am. J. Physiol 207, 291–297. [PubMed: 14205337]
23. Morrison SF, Madden CJ, and Tupone D. (2014). Central neural regulation of brown adipose tissue thermogenesis and energy expenditure. Cell Metab. 19, 741–756. [PubMed: 24630813]

24. Tan CL, and Knight ZA (2018). Regulation of Body Temperature by the Nervous System. Neuron 98, 31–48. [PubMed: 29621489]
25. Deem JD, Faber CL, Pedersen C, Phan BA, Larsen SA, Ogimoto K, Nelson JT, Damian V, Tran MA, Palmiter RD, et al. (2020). Cold-induced hyperphagia requires AgRP neuron activation in mice. Elife 9, e58764.
26. Yang S, Tan YL, Wu X, Wang J, Sun J, Liu A, Gan L, Shen B, Zhang X, Fu Y, and Huang J. (2021). An mPOA-ARC(AgRP) pathway modulates cold-evoked eating behavior. Cell Rep. 36, 109502.
27. Beutler LR, Chen Y, Ahn JS, Lin YC, Essner RA, and Knight ZA (2017). Dynamics of Gut-Brain Communication Underlying Hunger. Neuron 96, 461–475.e5. [PubMed: 29024666]
28. Chen Y, Lin YC, Kuo TW, and Knight ZA (2015). Sensory detection of food rapidly modulates arcuate feeding circuits. Cell 160, 829–841. [PubMed: 25703096]
29. Goldstein N, McKnight AD, Carty JRE, Arnold M, Betley JN, and Alhadeff AL (2021). Hypothalamic detection of macronutrients via multiple gut-brain pathways. Cell Metab. 33, 676–687.e5. [PubMed: 33450178]
30. Su Z, Alhadeff AL, and Betley JN (2017). Nutritive, Post-ingestive Signals Are the Primary Regulators of AgRP Neuron Activity. Cell Rep. 21, 2724–2736. [PubMed: 29212021]
31. Yoo E-S, Yu J, and Sohn JW (2021). Neuroendocrine control of appetite and metabolism. Exp. Mol. Med 53, 505–516. [PubMed: 33837263]
32. Kühnen P, Clément K, Wiegand S, Blankenstein O, Gottesdiener K, Martini LL, Mai K, Blume-Peytavi U, Gru€ters A, and Krude H. (2016). Proopiomelanocortin Deficiency Treated with a Melanocortin-4 Receptor Agonist. N. Engl. J. Med 375, 240–246. [PubMed: 27468060]
33. Kojima M, Hosoda H, Date Y, Nakazato M, Matsuo H, and Kangawa K. (1999). Ghrelin is a growth-hormone-releasing acylated peptide from stomach. Nature 402, 656–660. [PubMed: 10604470]
34. Shaw AM, Irani BG, Moore MC, Haskell-Luevano C, and Millard WJ (2005). Ghrelin-induced food intake and growth hormone secretion are altered in melanocortin 3 and 4 receptor knockout mice. Peptides 26, 1720–1727. [PubMed: 16005545]
35. Liu T, Kong D, Shah BP, Ye C, Koda S, Saunders A, Ding JB, Yang Z, Sabatini BL, and Lowell BB (2012). Fasting activation of AgRP neurons requires NMDA receptors and involves spinogenesis and increased excitatory tone. Neuron 73, 511–522. [PubMed: 22325203]
36. Yang Y, Atasoy D, Su HH, and Sternson SM (2011). Hunger states switch a flip-flop memory circuit via a synaptic AMPK-dependent positive feedback loop. Cell 146, 992–1003. [PubMed: 21925320]
37. Henry FE, Sugino K, Tozer A, Branco T, and Sternson SM (2015). Cell type-specific transcriptomics of hypothalamic energy-sensing neuron responses to weight-loss. Elife 4, e09800.
38. Bartos JA, Ulrich JD, Li H, Beazely MA, Chen Y, Macdonald JF, and Hell JW (2010). Postsynaptic clustering and activation of Pyk2 by PSD-95. J. Neurosci 30, 449–463. [PubMed: 20071509]
39. Giralt A, Brito V, Chevy Q, Simonnet C, Otsu Y, Cifuentes-Díaz C, de Pins B, Coura R, Alberch J, Ginés S, et al. (2017). Pyk2 modulates hippocampal excitatory synapses and contributes to cognitive deficits in a Huntington's disease model. Nat. Commun 8, 15592. [PubMed: 28555636]
40. Wei Q, Krolewski DM, Moore S, Kumar V, Li F, Martin B, Tomer R, Murphy GG, Deisseroth K, Watson SJ Jr., and Akil H. (2018). Uneven balance of power between hypothalamic peptidergic neurons in the control of feeding. Proc. Natl. Acad. Sci. USA 115, E9489–E9498. [PubMed: 30224492]
41. Vong L, Ye C, Yang Z, Choi B, Chua S Jr., and Lowell BB (2011). Leptin action on GABAergic neurons prevents obesity and reduces inhibitory tone to POMC neurons. Neuron 71, 142–154. 10.1016/j.neuron.2011.05.028. [PubMed: 21745644]
42. Garfield AS, Shah BP, Burgess CR, Li MM, Li C, Steger JS, Madara JC, Campbell JN, Kroeger D, Scammell TE, et al. (2016). Dynamic GABAergic afferent modulation of AgRP neurons. Nat. Neurosci 19, 1628–1635. 10.1038/nn.4392. [PubMed: 27643429]
43. Krashes MJ, Shah BP, Madara JC, Olson DP, Strochlic DE, Garfield AS, Vong L, Pei H, Watabe-Uchida M, Uchida N, et al. (2014). An excitatory paraventricular nucleus to AgRP neuron circuit that drives hunger. Nature 507, 238–242. [PubMed: 24487620]

44. Grzelka K, Wilhelms H, Dodt S, Dreisow ML, Madara JC, Walker SJ, Wu C, Wang D, Lowell BB, and Fenselau H. (2023). A synaptic amplifier of hunger for regaining body weight in the hypothalamus. Cell Metab 35, 770–785.e5. [PubMed: 36965483]

45. Atasoy D, Betley JN, Su HH, and Sternson SM (2012). Deconstruction of a neural circuit for hunger. Nature 488, 172–177. 10.1038/nature11270. [PubMed: 22801496]

46. Roseberry AG, Liu H, Jackson AC, Cai X, and Friedman JM (2004). Neuropeptide Y-mediated inhibition of proopiomelanocortin neurons in the arcuate nucleus shows enhanced desensitization in ob/ob mice. Neuron 41, 711–722. 10.1016/s0896-6273(04)00074-1. [PubMed: 15003171]

47. Furigo IC, Teixeira PDS, de Souza GO, Couto GCL, Romero GG, Perelló M, Frazaõ R, Elias LL, Metzger M, List EO, et al. (2019). Growth hormone regulates neuroendocrine responses to weight loss via AgRP neurons. Nat. Commun 10, 662. [PubMed: 30737388]

48. Srisai D, Yin TC, Lee AA, Rouault AAJ, Pearson NA, Grobe JL, and Sebag JA (2017). MRAP2 regulates ghrelin receptor signaling and hunger sensing. Nat. Commun 8, 713. [PubMed: 28959025]

49. Chen T-W, Wardill TJ, Sun Y, Pulver SR, Renninger SL, Baohan A, Schreiter ER, Kerr RA, Orger MB, Jayaraman V, et al. (2013). Ultrasensitive fluorescent proteins for imaging neuronal activity. Nature 499, 295–300. [PubMed: 23868258]

Highlights

- MC3R is required for normal AgRP neuron activation by fasting, cold, or ghrelin
- MC3R in AgRP neurons is required for activation of the neurons by fasting or ghrelin
- MC3R in AgRP neurons regulates genes involved in hormonal and neuronal activation

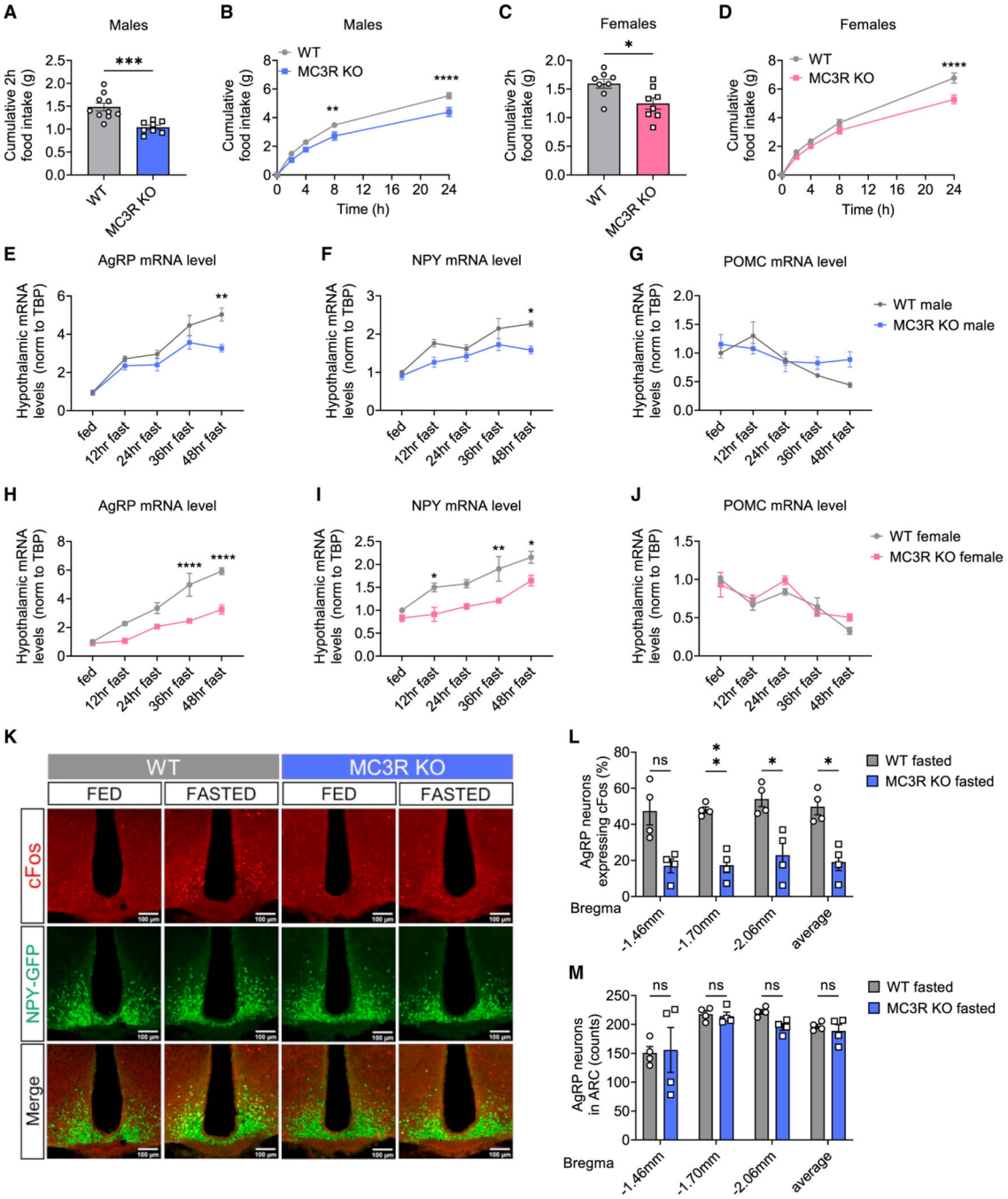

Figure 1. MC3R is required for the activation of AgRP neurons by fasting

(A−D) 2- (A and C) and 24-h (B and D) food intake of WT and MC3R KO male and female mice following a 24-h fast (n = 8–10 mice for all groups).

(E−J) qPCR analysis of hypothalamic AGRP, NPY, and POMC mRNA levels in WT and MC3R KO male and female mice over a 48-h-fasting time course (n = 3–9 mice for all groups).

(K−M) Representative images of GFP and cFos immunostaining, and quantifications of the percentage of cFos-positive GFP cells and the number of GFP cells in the ARC of 24-h-fasted WT and MC3R KO NPY-GFP male mice.
Scale bar, 100 μm (n = 4 mice for all groups). Data are plotted as mean, and all error bars represent the SEM. ns, non-significant; *p < 0.05; **p < 0.01; ***p < 0.001; ****p < 0.0001 in unpaired Student's t test and two-way ANOVA with Sidak's post hoc test.

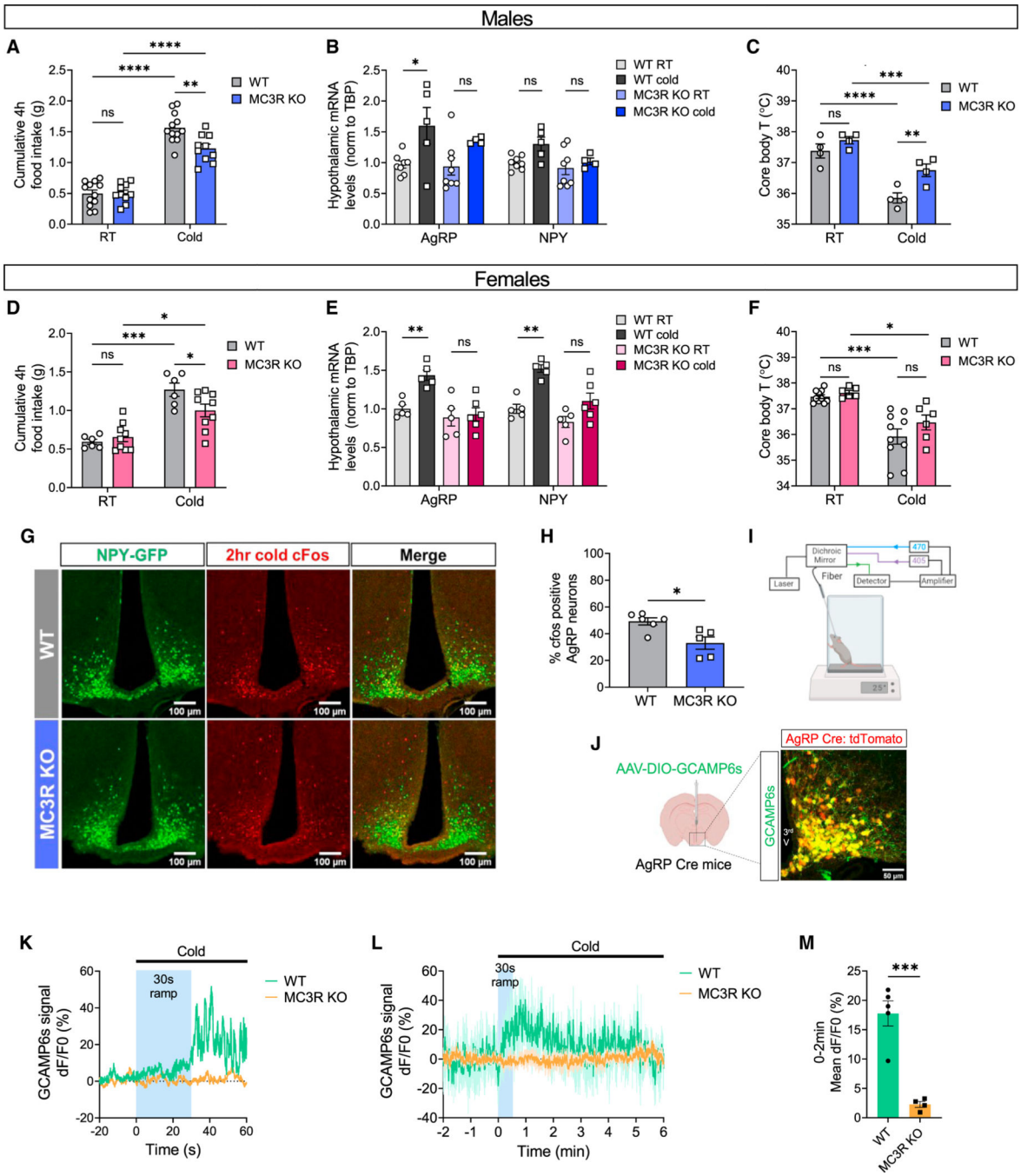

Figure 2. MC3R is required for the activation of AgRP neurons in response to cold

(A and D) 4-h food intake of WT and MC3R KO male and female mice under room temperature (RT; 22°C) or cold exposure (4°C) (n = 6–12 mice for all groups). (B, C, E, and F) qPCR analysis of hypothalamic AGRP and NPY mRNA levels (B and E) and measurement of rectal temperature (C and F) in WT and MC3R KO male and female mice under RT or following 4-h cold exposure (n = 4–10 mice for all groups).

(G and H) Representative images of GFP and cFos immunostaining, and quantifications of the percentage of cFos-positive GFP cells in the ARC of WT and MC3R KO NPY-GFP male mice following 2-h cold exposure. Scale bar, 100 mm (n = 5–6 mice for each group).
(I) Schematic showing the setup of fiber photometry on a cold plate.
(J) Validation of Cre-dependent GCAMP6s viral expression in AgRP Cre:tdTomato mice. Scale bar, 50 μm.
(K) Representative calcium signal traces from one WT mouse and one MC3R KO male mouse in response to cold exposure for 60 s. −20 to 0 s, 22°C; 0 to 60 s, 12°C, with 30-s temperature ramp.
(L and M) Traces and quantifications of averaged dF/F0 (%) GCaMP6s signal in AgRP neurons in WT and MC3R KO male mice during prolonged cold exposure. −2 to 0 min, 22°C; 0 to 6 min, 12°C, with 30-s temperature ramp (n = 5 mice for WT and n = 4 for MC3R KO groups).
Data are plotted as mean, and all error bars represent the SEM. ns, non-significant; *p < 0.05; **p < 0.01; ***p < 0.001; ****p < 0.0001 in unpaired Student's t test and two-way ANOVA with Sidak's post hoc test.

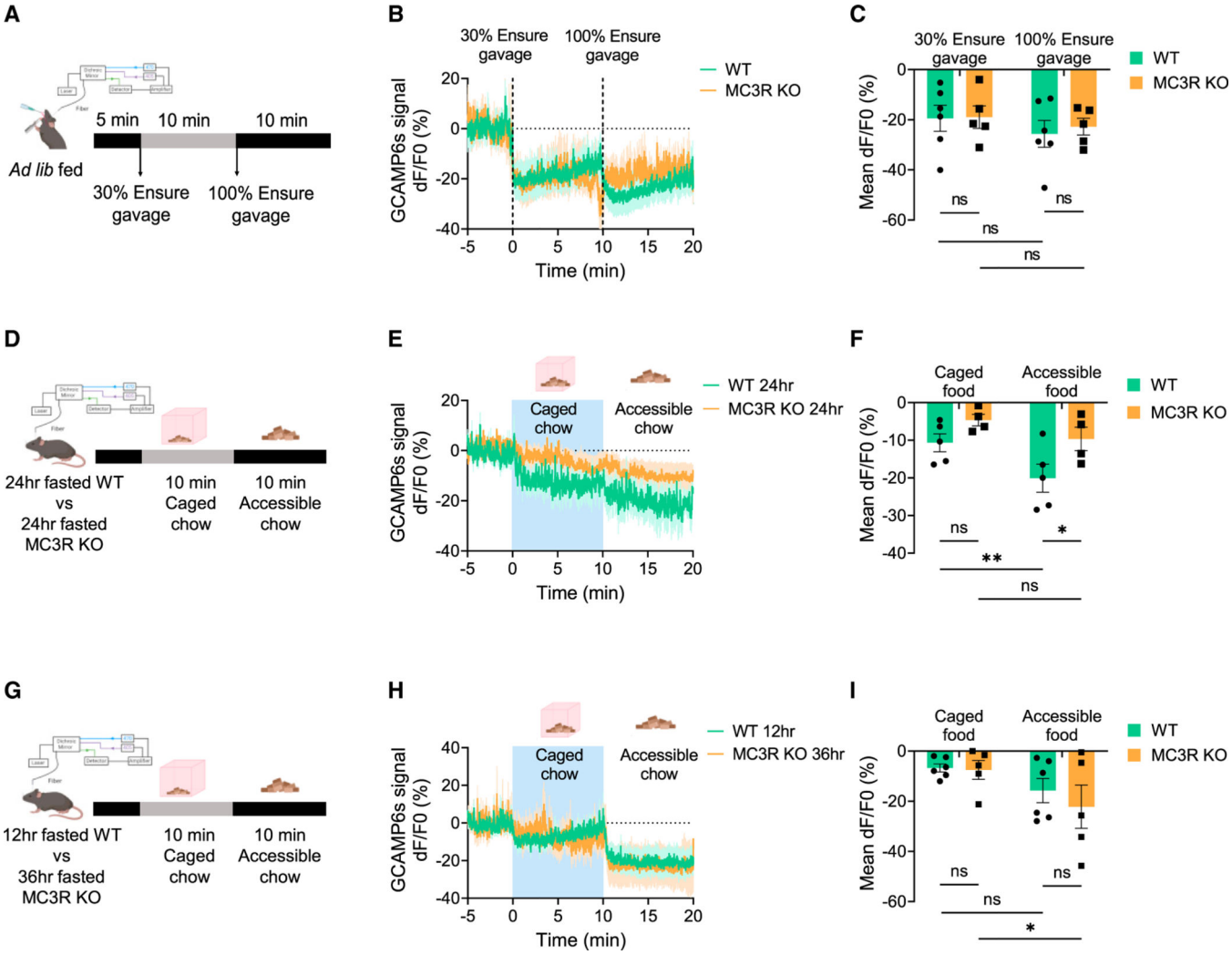

Figure 3. MC3R is not required for the inhibition of AgRP neurons by sensory detection of nutrients or food cues

(A) Schematic showing the setup of fiber photometry in *ad lib*-fed male mice in response to 30% or 100% Ensure gavage.

(B and C) Traces and quantifications of averaged dF/F0 (%) GCaMP6s signal in AgRP neurons in *ad lib*-fed WT or MC3R KO male mice in response to 30% or 100% Ensure gavage (n = 5–6 mice for each group).

(D) Schematic showing the setup of fiber photometry in 24-h-fasted WT or MC3R KO male mice in response to caged or accessible food cues. (E and F) Traces and quantifications of averaged dF/F0 (%) GCaMP6s signal in AgRP neurons in 24-h-fasted WT or MC3R KO male mice in response to caged or accessible food cues (n = 4–5 mice for each group).

(G) Schematic showing the setup of fiber photometry in 12-h-fasted WT or 36-h-fasted MC3R KO male mice in response to caged or accessible food cues. (H and I) Traces and quantifications of averaged dF/F0 (%) GCaMP6s signal in AgRP neurons in 12-h-fasted WT or 36-h-fasted MC3R KO male mice in response to food cues (n = 5–6 mice for each group). Data are plotted as mean, and all error bars represent the SEM. ns, non-significant; *p < 0.05; **p < 0.01 in two-way ANOVA with Sidak's post hoc test.

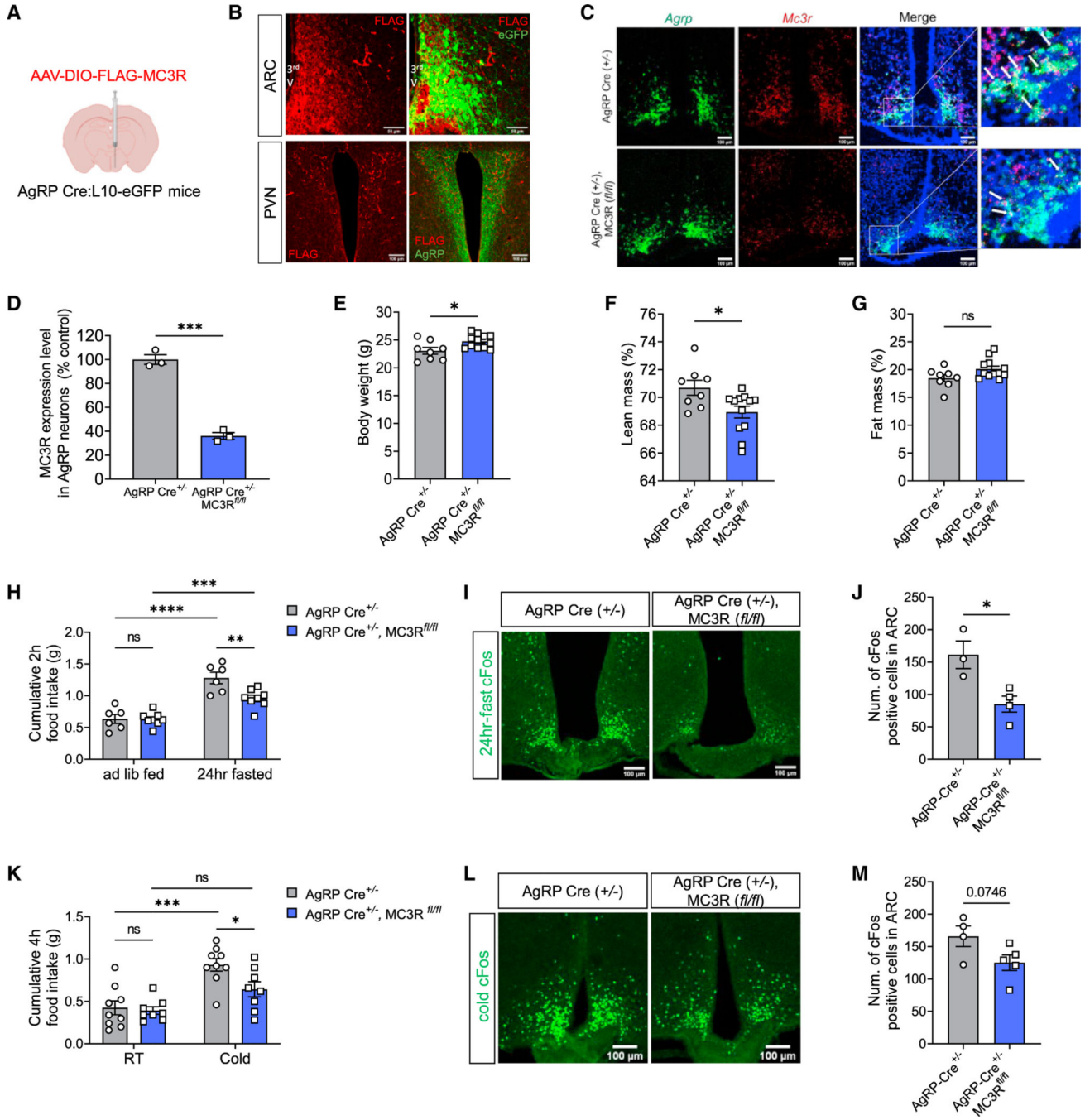

Figure 4. MC3R deletion in AgRP neurons impairs energy deficiency sensing

(A and B) Validation of Cre-dependent MC3R-FLAG viral expression in AgRP Cre:L10-EGFP mice by immunostaining against FLAG, EGFP, and AgRP. Scale bar, 50 μm for the ARC and 100 μm for the PVN.

(C and D) RNAscope analysis of *Mc3r* and *Agrp* mRNA expression, and quantifications of the percentage of AgRP-positive cells coexpressing MC3R in the ARC of AgRP-Cre and AgRP-specific MC3R KO male mice. Scale bar, 100 μm (n = 3 mice for each group).

(E−G) Body weight and body composition of AgRP-Cre and AgRP-specific MC3R KO male mice (n = 8 mice for AgRP-Cre and n = 12 for AgRP-specific MC3R KO groups).
(H) 2-h food intake of AgRP-Cre and AgRP-specific MC3R KO male mice following a 24-h fast (n = 6 mice for AgRP-Cre and n = 8 for AgRP-specific MC3R KO groups).
(I and J) Representative images of cFos immunostaining, and quantifications of cFos-positive cell number in the ARC of 24-h-fasted AgRP-Cre and AgRP-specific MC3R KO male mice. Scale bar, 100 μm (n = 3 mice for AgRP-Cre and n = 4 for AgRP-specific MC3R KO groups).
(K) 4-h food intake of AgRP-Cre and AgRP-specific MC3R KO male mice under RT (22°C) or cold exposure (4°C) (n = 9 mice for AgRP-Cre and n = 8 for AgRP-specific MC3R KO groups).
(L and M) Representative images of cFos immunostaining, and quantifications of cFos-positive cell number in the ARC of cold-treated AgRP-Cre and AgRP-specific MC3R KO male mice. Scale bar, 100 μm (n = 4 mice for AgRP-Cre and n = 5 for AgRP-specific MC3R KO groups).
Data are plotted as mean, and all error bars represent the SEM. ns, non-significant; *$p < 0.05$; **$p < 0.01$; ***$p < 0.001$; ****$p < 0.0001$ in unpaired Student's t test and two-way ANOVA with Sidak's post hoc test.

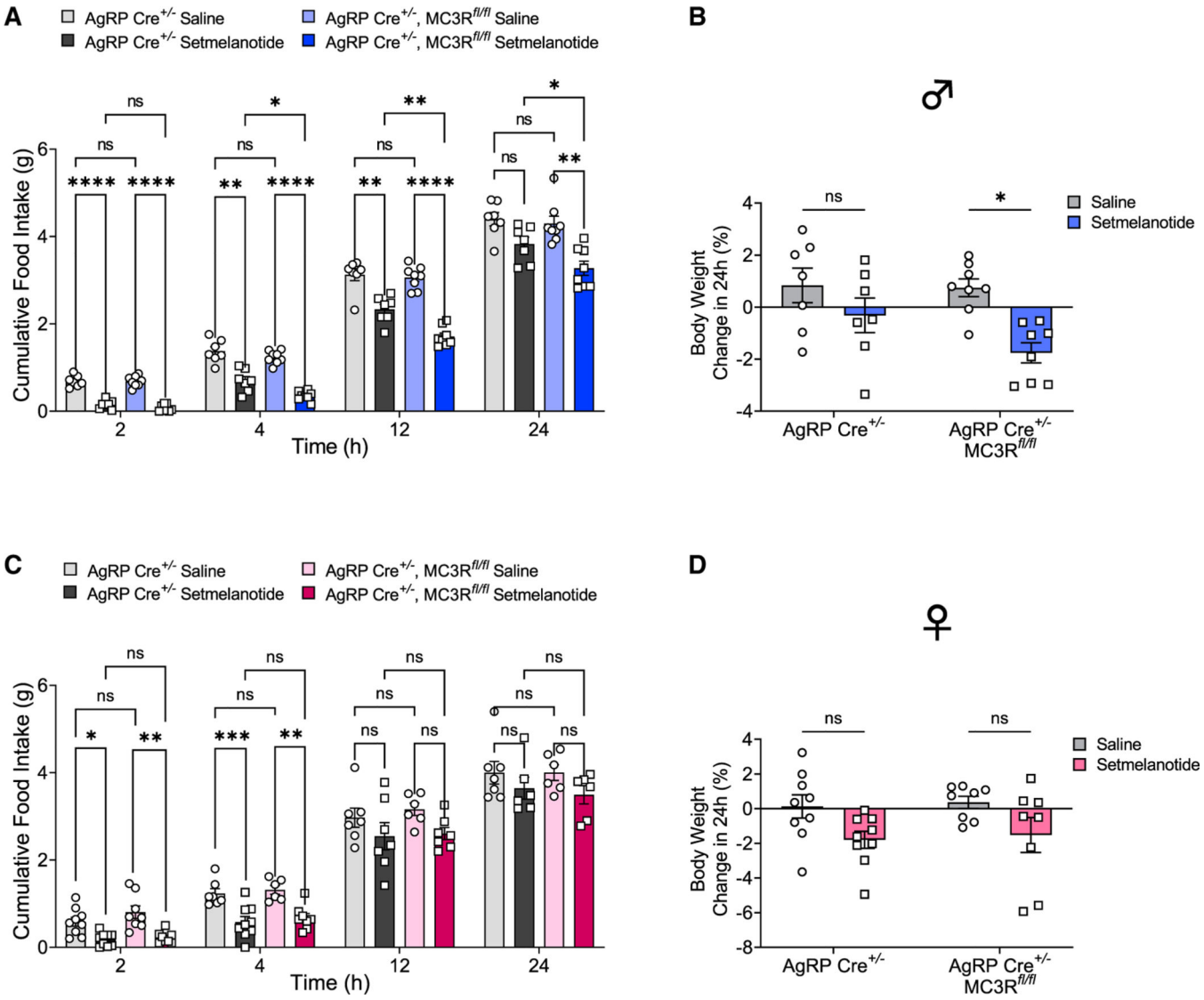

Figure 5. MC3R regulates downstream MC4R-mediated anorexigenic activity thorough its action in AgRP neurons

(A and B) Food intake and percentage change of 24-h body weight in AgRP-Cre and AgRP-specific MC3R KO male mice given saline or setmelanotide injection (2 mg/kg, i.p.) (n = 7–8 mice for each group).

(C and D) Food intake and percentage change of 24-h body weight in AgRP-Cre and AgRP-specific MC3R KO female mice given saline or setmelanotide injection (2 mg/kg, i.p.) (n = 8–9 mice for each group).

Data are plotted as mean, and all error bars represent the SEM. ns, non-significant; *p < 0.05; **p < 0.01; ***p < 0.001; ****p < 0.0001 in two-way ANOVA with Sidak's post hoc test.

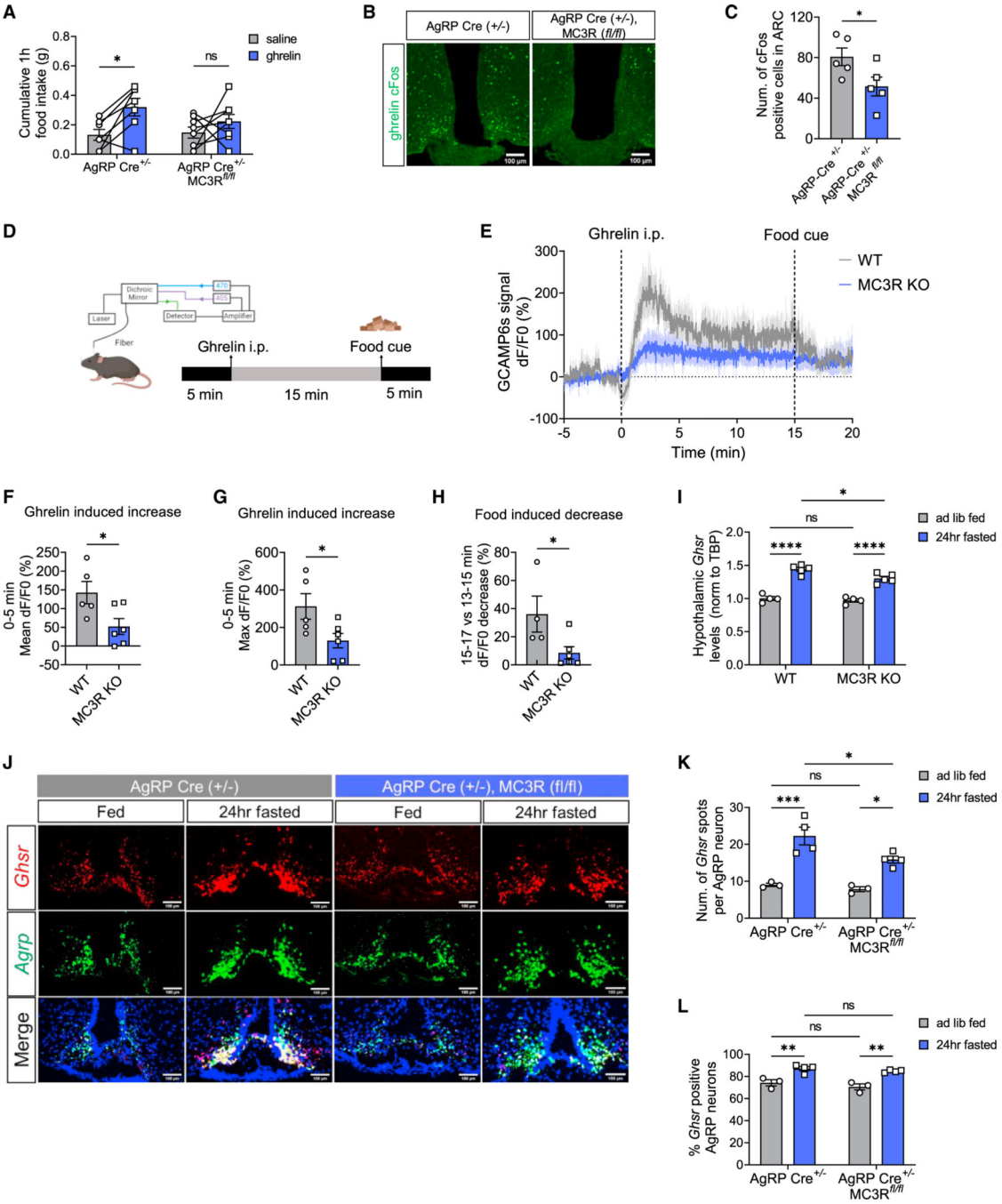

Figure 6. MC3R is required for the orexigenic action of ghrelin on AgRP neurons

(A) 1-h food intake of AgRP-Cre and AgRP-specific MC3R KO male mice given saline or ghrelin injection (1.6 mg/kg, i.p.) (n = 7–8 mice for all groups).

(B and C) Representative images of cFos immunostaining, and quantifications of cFos-positive cell number in the ARC of AgRP-Cre and AgRP-specific MC3R KO male mice in response to saline or ghrelin injection. Scale bar, 100 μm (n = 4–5 mice for each group).

(D) Schematic showing the time course of ghrelin injection and food presence in fiber photometry experiment

(E−H) Traces and quantifications of averaged dF/F0 (%) GCaMP6s signal in AgRP neurons in WT and MC3R KO male mice in response to ghrelin and food cue (n = 4–5 mice for all groups).

(I) qPCR analysis of hypothalamic GHSR mRNA levels in fed versus 24-h-fasted WT and MC3R KO male mice (n = 3–5 mice for all groups).

(J−L) RNAscope analysis of *Agrp* and *Ghsr* mRNA expression, and quantifications of the number of *Ghsr* transcripts in each AgRP neuron and the percentage of AgRP neurons coexpressing *Ghsr* in the ARC of fed versus 24-h-fasted AgRP-Cre and AgRP-specific MC3R KO male mice. Scale bar, 100 μm (n = 3–4 mice for all groups).

Data are plotted as mean, and all error bars represent the SEM. ns, non-significant; *p < 0.05; **p < 0.01; ***p < 0.001; ****p < 0.0001 in unpaired Student's t test and two-way ANOVA with Sidak's post hoc test.

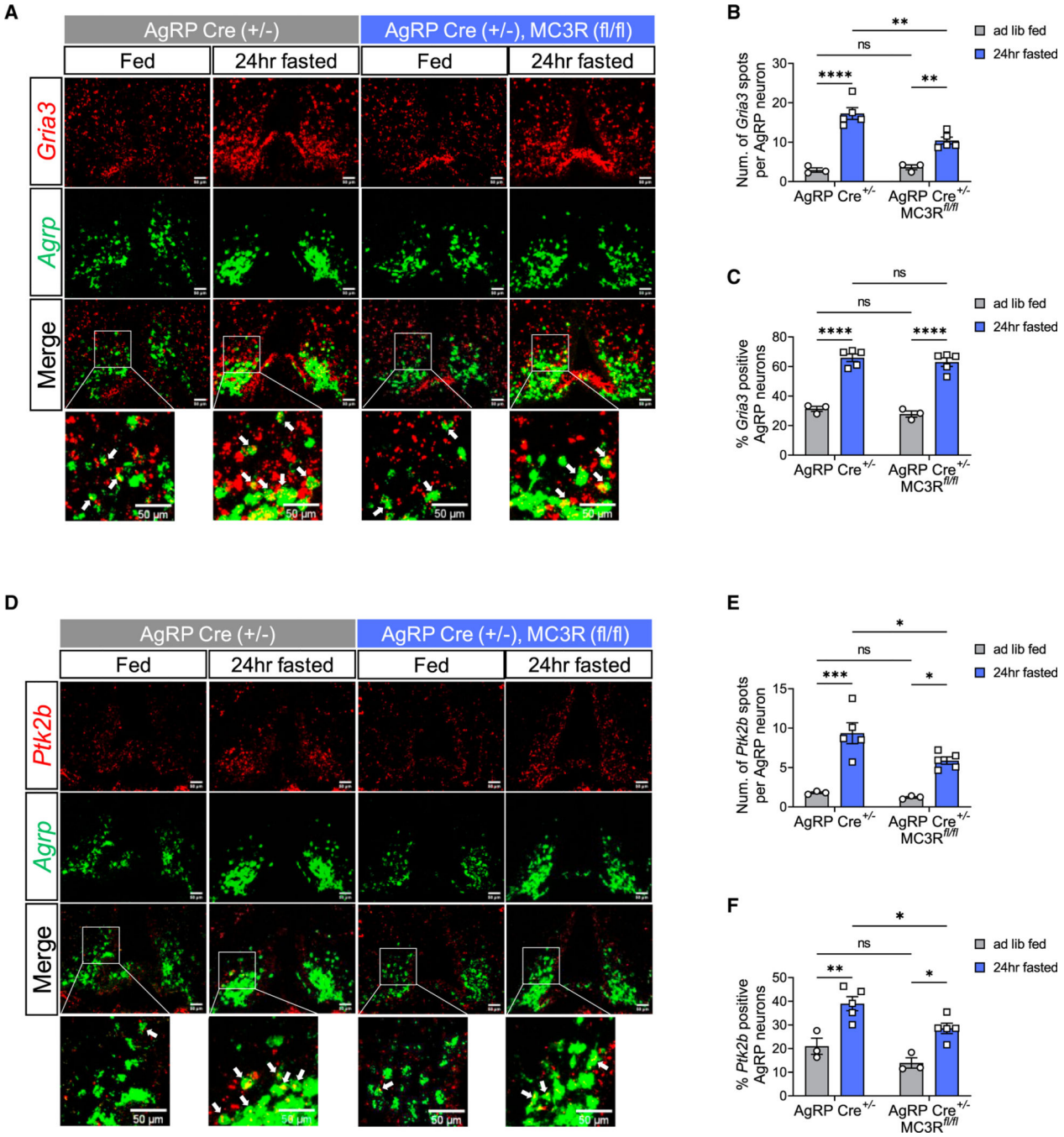

Figure 7. MC3R is required for excitatory synapse-associated gene expression in AgRP neurons

(A–C) RNAscope analysis of *Agrp* and *Gria3* mRNA expression, and quantifications of the number of *Gria3* transcripts in each AgRP neuron and the percentage of AgRP neurons coexpressing *Gria3* in the ARC of fed versus 24-h-fasted AgRP-Cre and AgRP-specific MC3R KO male mice. Scale bar, 50 μm (n = 3–5 mice for all groups).

(D–F) RNAscope analysis of *Agrp* and *Ptk2b* mRNA expression, and quantifications of the number of *Ptk2b* transcripts in each AgRP neuron and the percentage of AgRP neurons

coexpressing *Ptk2b* in the ARC of fed versus 24-h-fasted AgRP-Cre and AgRP-specific MC3R KO male mice. Scale bar, 50 μm (n = 3–5 mice for all groups).

Data are plotted as mean, and all error bars represent the SEM. ns, non-significant; *p < 0.05; **p < 0.01; ***p < 0.001; ****p < 0.0001 in unpaired Student's t test and two-way ANOVA with Sidak's post hoc test.

KEY RESOURCES TABLE

REAGENT or RESOURCE	SOURCE	IDENTIFIER
Antibodies		
Rabbit anti-Fos (9F6) antibody	Cell Signaling	Cat# 2250S; RRID:AB_2247211
Chicken anti-GFP antibody	Aves Labs	Cat# GFP-1020; RRID:AB_2307313
Mouse anti-FLAG M2 antibody	Sigma	Cat# F1804; RRID: AB_262044
Rabbit anti-AgRP antibody	Phoenix Pharmaceuticals	Cat# H-003–57; RRID: AB_2313909
Goat anti-Rabbit IgG (H + L), Alexa Fluor 488	Thermo Fisher Scientific	Cat# A32731; RRID: AB_2633280
Goat anti-Rabbit IgG (H + L), Alexa Fluor 555	Thermo Fisher Scientific	Cat# A21428; RRID:AB_2535849
Goat anti-Chicken IgY (H + L), Alexa Fluor 488	Thermo Fisher Scientific	Cat# A11039; RRID: AB_2534096
Goat anti-mouse 594 IgG (H + L), Alexa Fluor 555	Thermo Fisher Scientific	Cat# A21422; RRID: AB_2535844
Bacterial and virus strains		
pAAV5-Syn-Flex-GCaMP6s-WPRE-SV40	(Chen et al.)[49]	Cat# 100845-AAV5
rAAV2-U6-scrShRNA-CMV-eGFP	Vector Core, University of Michigan	N/A
rAAV2-U6-MC3R-ShRNA-CMV-eGFP	Vector Core, University of Michigan	N/A
rAAV9-CMV-FLAG-MC3R	Vector Core, University of Michigan	N/A
Chemicals, peptides, and recombinant proteins		
Setmelanotide	Vivitide	N/A
Ghrelin (rat)	Tocris Bioscience	Cat# 1465
High-Capacity cDNA Reverse Transcription Kit	Applied Biosystems	Cat# 4368814
RNAscope® H2O2 and Protease Reagents	Advanced Cell Diagnostics	Cat# 322381
RNAscope® Multiplex Fluorescent Detection Reagents v2	Advanced Cell Diagnostics	Cat# 323110
RNAscope® Wash Buffer Reagents	Advanced Cell Diagnostics	Cat# 310091
RNAscope® Multiplex TSA Buffer	Advanced Cell Diagnostics	Cat# 322809
Mm-Mc3r-C1	Advanced Cell Diagnostics	Cat# 412541
Mm-Gria3-C1	Advanced Cell Diagnostics	Cat# 426251
Mm-Agrp-C2	Advanced Cell Diagnostics	Cat# 400711-C2
Mm-Ghsr-C3	Advanced Cell Diagnostics	Cat# 426141-C3

REAGENT or RESOURCE	SOURCE	IDENTIFIER
Mm-Ptk2b-C3	Advanced Cell Diagnostics	Cat# 506861-C3
Opal™ 520 Reagent Pack	Akoya Biosciences	Cat# FP1487001KT
Opal™ 570 Reagent Pack	Akoya Biosciences	Cat# FP1488001KT
Opal™ 690 Reagent Pack	Akoya Biosciences	Cat# FP1497001KT
Critical commercial assays		
Leptin ELISA Kit	Crystal Chem	Cat# 90030
Total T4 ELISA kit	Diagnostic Automation	Cat# 3149–16
Experimental models: Organisms/strains		
Mouse: C57BL/6J (B6/J)	Jackson Laboratory	Cat# Jax: 000664
Mouse: AgRP-IRES-Cre	Jackson Laboratory	Cat# Jax: 012899
Mouse: NPY-hrGFP	Jackson Laboratory	Cat# Jax: 006417
Mouse: Ai14	Jackson Laboratory	Cat# Jax: 007914
Mouse: EGFP-L10a	Jackson Laboratory	Cat# Jax: 024750
Mouse: MC3R $^{flox/flox}$	This paper	N/A
Oligonucleotides		
qPCR primer Ms-Ghsr-Fwd: GACCAGAACCACAAACAGACAG	Sigma	N/A
qPCR primer Ms-Ghsr-Rev: GGCTCGAAAGACTTGGAAAA	Sigma	N/A
Software and algorithms		
GraphPad Prism 9	GraphPad	https://www.graphpad.com/
ImageJ	NIH ImageJ	https://imagej.nih.gov/ij/
MATLAB 2022a	MathWorks	https://www.mathworks.com/products/matlab.html
LAS X	Leica	https://www.leica-microsystems.com
FED3 device	Open Ephys	https://open-ephys.org/fed3/fed3